# The $C_{60}$ cluster as a new form of carbon

A. V. Eletskiĭ and B. M. Smirnov

*Institute of High Temperatures, Academy of Sciences of the USSR, Moscow*

(Submitted February 4, 1991)
Usp. Fiz. Nauk **161**, 173–192 (July 1991)

The parameters of a cluster consisting of 60 carbon atoms are presented. Among these are structural, geometric, optical, and energy parameters. Methods of generating $C_{60}$ clusters are investigated. $C_{60}$ is considered as one of the forms of soot that is formed in flames. Properties of a crystal consisting of clusters of $C_{60}$ are analyzed. In particular, such a crystal has a density of 1.3 g/cm$^3$ and a melting point at about 500 K.

*The Structure of a $C_{60}$ Cluster; The Generation of $C_{60}$ Clusters; The Breakup of Carbon Clusters; Spectroscopy of $C_{60}$; Soot and the $C_{60}$ Cluster; Macrostructures Consisting of $C_{60}$ Clusters.*

## INTRODUCTION

Research on clusters,[1)] systems consisting of a finite number of bound atoms, indicates the effect of the structure of a cluster on its stability.[1,2] This fact appears in the existence of magic numbers, the number of atoms in a cluster for which it has the greatest stability. The actual expression of the indicated fact is that the intensity of the flux of charged clusters with the magic number emerging from a source is higher than the corresponding fluxes of clusters with one less or one more atom in them. A definite set of magic numbers corresponds to each element or kind of clusters, in accordance with the structure of the cluster. For example, 13, 16, 19, 55, 71, 87, and 147 are the magic numbers for xenon,[3–6] part of which corresponds to the icosahedral structure that is characteristic for a crystal of an inert gas.

One of the magic numbers for carbon is $n = 60$. A $C_{60}$ cluster has the structure of the cover of a soccer ball (see Fig. 1)[7] and is easily distinguished among clusters with neighboring $n$ values by its stability. The carbon atoms occupy the vertices of 20 regular hexagons and of 12 regular pentagons, which cover the surface of a sphere in such a manner that each pentagon has common boundaries only with hexagons, and each hexagon borders on three pentagons and three hexagons. The closed nature of the structure of a cluster leads to a high inertness, i.e., to a low reaction capability. The increased stability and high inertness of a $C_{60}$ cluster enables one to create conditions such that, during the vaporization of graphite by laser radiation, the vaporized carbon mainly consists of $C_{60}$ clusters. One can precipitate such clusters onto a substrate and convert the carbon by this method into a new stable state. One obtains by this method a new form of carbon, which is a new, interesting material.

However, interest in the $C_{60}$ cluster is not limited to the problem of creating new materials. As a carbon compound with increased stability, it can play a definite role in the formation of soot, a product of the incomplete combustion of carbonaceous compounds. In particular, in flames of organic fuels with high radiation intensities, soot particles, which are an intermediate product of the process of oxidation, emit light and continue to burn. The presence of the $C_{60}$ cluster in soot may show up in the optical properties of the flame, since by virtue of its structure, the $C_{60}$ cluster differs in optical properties from other varieties of soot.

Although the question of the existence of the $C_{60}$ cluster was discussed repeatedly earlier (see, for example, Refs. 9 through 14), the history of modern investigations began with Ref. 15, in which the $C_{60}$ cluster was established as a cluster with a magic number of atoms in it. This served as the start for investigating different properties of this cluster.[16–21] The next step was taken in 1990 and is connected with the creation of the technology for producing $C_{60}$ clusters, which enabled one to process graphite carbon mainly into $C_{60}$ clusters.[22–27] This possibility enables one to distinguish this cluster among clusters with magic numbers and to consider it as a new form of carbon. The high inertness of $C_{60}$ clusters enables one to retain them really forever. This opens the possibility of forming a crystal from $C_{60}$ clusters. Thus, $C_{60}$ clusters are a new and stable form of carbon.

Everything that has been said attracts the attention of researchers to the $C_{60}$ cluster and requires a more attentive analysis of its properties. Information on modern research on the $C_{60}$ cluster is collected in this review, and its properties and the processes in which it takes part are analyzed.

## 2. THE STRUCTURE OF A $C_{60}$ CLUSTER

A carbon atom has a $s^2p^2$ electron shell. This shell provides the optimal structure for carbon when neighboring atoms form pentagons or hexagons.[2)] Such a structure also occurs in modifications of solid carbon, diamond and graph-

FIG. 1. The structure of a $C_{60}$ cluster.

 0038-5670/91/070616-10$01.00  

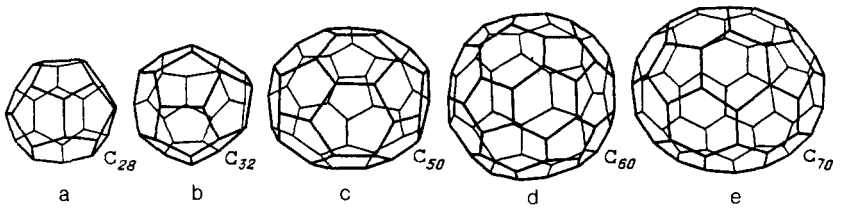


FIG. 2. Clusters of carbon with closed structures formed from pentagonal and hexagonal carbon rings. The number of atoms in the clusters are: a) 28; b) 32; c) 50; d) 60; and e) 70.[7] These numbers are magic ones for carbon clusters.

ite; it is optimal for the most stable carbon clusters. All these clusters have the structure of a closed surface on which the carbon atoms are located. This closed surface is covered with hexagons and pentagons. A family of such clusters is represented in Fig. 2;[7] one must also include in it the $C_{60}$ cluster represented in Fig. 1.

The vaporization of graphite is the most efficient method for obtaining $C_{60}$ clusters. Obviously, the structures of a $C_{60}$ cluster and graphite are analogous. Let us use this analogy to analyze the structure of a $C_{60}$ cluster.

The structure of graphite is represented in Fig. 3. Graphite has a layered structure (see Refs. 28 and 29); each layer is covered with hexagons. The length of a side of a hexagon is 0.142 nm, the distance between layers is 0.335 nm, and moreover, the atoms of neighboring layers are not situated one above the other, but are displaced by half the lattice constant. It is reasonable to think that a $C_{60}$ cluster contains the same hexagons as does graphite. Let us determine the radius of a cluster. Let us cut the cluster with a plane which passes through its center and divides the cluster into symmetric parts. This plane will cut four hexagons and four pentagons in half, and will pass through two sides of a hexagon. The perimeter of the figure of the intersection equals $10a + 4b \approx 16.16a$, where $a = 0.142$ nm, the length of the side of a hexagon, and $b \approx 1.54a$ is the altitude of a pentagon. If one assumes that the perimeter is the same as the circumference $2\pi R$ of the circle which is formed when the sphere in which the cluster is inscribed is cut by the plane, then the radius of the sphere equals $R = 2.57a$. The replacement of the actual segments of the figure of the intersection by arcs increases the circumference of the circle somewhat, which turns out to equal $16.46a$. Accordingly, the radius of the sphere is $R = 2.62a = 0.37$ nm. Even though this operation is not entirely correct, since only the the vertices of the figures are located on the surface of the sphere, its accuracy is estimated at 1%, which is not beyond the error of the model.

The connection between the structure of graphite and the structure of a closed carbon cluster also appears in the cluster formation mechanism. For moderate heating of graphite, the connection between individual graphite layers is broken, and a vaporized layer is broken up into individual fragments. These fragments are combinations of hexagons, and the cluster formation then proceeds from them. One can suggest different models by which way one can collect a cluster from the fragments. To form a $C_{60}$ cluster under consideration by the simplest method, it would appear that one could take 10 hexagons containing 60 atoms and join them in a closed structure. However, this is impossible to do for this structure without cutting up some hexagons. First of all, this is explained by the fact that, although a plane surface is easily covered by regular hexagons, a closed spherical surface whose radius is comparable in length with the side of a hexagon cannot be covered by them. Besides, it is impossible in this structure to single out 10 hexagons which do not have common vertices with each other. However, this structure allows an assembly of six independent double hexagons, each of which contains 10 atoms. Evidently this is the simplest method of assembly. This method can be modified if one assembles the cluster from fragments consisting of double hexagons. In particular, one of such fragments is represented in Fig. 4. The $C_{60}$ cluster under consideration consists of two fragments represented in this figure.

The transformation of a plane structure into a three-dimensional one is a significant element of an assembly of clusters with a closed structure. A typical case of such a transformation in the assembly of a three-dimensional cluster is shown in Fig. 5. This occurs as the result of closing the carbon bonds and leads to the formation of spatial pentagonal and hexagonal configurations of carbon. This process can then be continued to create also more complicated clusters (see Fig. 6). It is significant here that the assembly of clusters is accompanied by the joining of whole fragments which contain hexagonal configurations of carbon, but not by the joining of individual atoms. This is a fundamental feature of carbon, which is significant not only in forming closed clusters of carbon, but also soot.

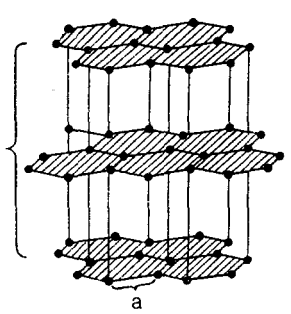


FIG. 3. The structure of graphite.

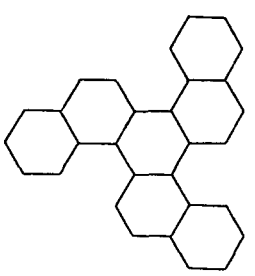

FIG. 4. A fragment of graphite which can form half of a $C_{60}$ cluster.

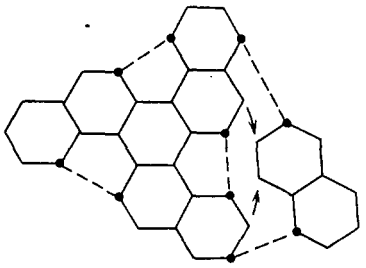

FIG. 5. The nature of the formation of part of a closed carbon cluster from graphite fragments. The joining of two fragments is shown. A large fragment consisting of seven hexagons (30 atoms) is bent into a three-dimensional structure such that the dashed lines close the corresponding sides of a pentagon. Next a fragment consisting of two hexagons (10 atoms) forms, with the large fragment, a hexagon (which is closed by the arrows) and two pentagons (which are closed by the dashed lines). Part of a $C_{60}$ cluster containing 40 atoms, six closed pentagons, and 10 closed hexagons is created by this method from these fragments. One can obtain a $C_{60}$ cluster from this fragment by adding to it two more fragments which are double hexagons.

### 3. THE GENERATION OF $C_{60}$ CLUSTERS

Since the structure of the cluster under consideration is similar to the structure of graphite, the best method for obtaining these clusters is based on the thermal vaporization of graphite. A typical mass-spectrum of the charged clusters which are formed during the laser vaporization of graphite is presented in Fig. 7.[21] As is evident, clusters with an even number of carbon atoms are more stable.

In choosing the best conditions for generating $C_{60}$ clusters, one must take into account that the heating of the graphite must be moderate. Then it will allow breaking the bonds between the individual layers of graphite, but will not lead to the dissociation of the vaporized carbon into individual atoms. Here the vaporized graphite will consist of fragments which contain hexagonal configurations of carbon atoms. The assembly of a $C_{60}$ cluster also occurs from these fragments.

Graphite vaporization which is accompanied by the formation of a flux of such fragments from its surface occurs either as the result of resistance heating of a graphite electrode[26] or as the result of laser irradiation of a graphite surface.[23] The buffer gas, helium is commonly used as such a gas, plays a significant role here. The main role of the helium is evidently connected with cooling the fragments, which obviously have a high degree of vibrational excitation that hinders the formation of stable structures from these fragments. Besides, the helium atoms carry off the energy which is given off upon the joining of fragments. The advantage of helium over other types of buffer gas is connected with the high efficiency of damping vibrationally excited molecules that is typical for this atom. Clearly there exists an optimal buffer gas pressure, for the assembly of carbon fragments is hindered at high pressures. Experiment shows that the optimal helium pressure is in the range from 50 Torr to 100 Torr.

As is evident from Fig. 7, the flux of carbon fragments which is formed as a result of the thermal vaporization of a graphite surface contains, along with $C_{60}$ and $C_{70}$ clusters, a large number of lighter clusters with even numbers of carbon atoms. Under suitable conditions, a significant fraction of these clusters is converted into $C_{60}$ and $C_{70}$ clusters. For this, one must hold the carbon condensate for several hours either at a temperature from 500 °C to 600 °C or at a lower temperature in the form of a solution in a non-polar solvent. The kinetics of the formation of $C_{60}$ and $C_{70}$ under the indicated conditions have not been determined in detail; however, one may suppose that they include a great number of processes for forming and breaking carbon bonds. The chain of such processes is cut short as a result of the formation of clusters with increased stability. Thereby, after the passage of a sufficiently long time, practically all the carbon condensate is converted into the stable form of $C_{60}$ and $C_{70}$. Thus, the procedure for obtaining a carbon condensate with a high content of $C_{60}$ contains two stages, the first of which consists of thermal vaporization or pulverization of a graphite surface, and the second consists of joining the products of such pulverization into stable formations. The indicated conditions determine the degree of complexity of the technology for obtaining a carbon condensate with a high relative $C_{60}$ content.

Thus, in Refs. 23, 24, and 25, which are devoted to investigating the Raman scattering spectra of $C_{60}$ clusters, the carbon condensate which was formed as a result of the resistance heating of a graphite rod (the degree of purity of the graphite was 99.99%) was collected on a glass disk in helium at 100 Torr pressure. Approximately 20 mg of fine black powder obtained here, which was scraped off the disk in air, was placed into a small cell made of stainless steel and having a nozzle with a 2 mm inner diameter. The small cell was placed in a chamber, the pressure in which was maintained at the $10^{-5}$ Torr level. Heating the cell to a temperature of 500 °C to 600 °C led to an outflow of small carbon condensate particles from the nozzle, which were then collected on a thin tungsten band and formed a layer several microns thick on it. The mass spectrum of these small particles was investigated by means of surface vaporization by the action of a KrF-laser with a pulse energy of 60 $\mu$J and a beam diam-

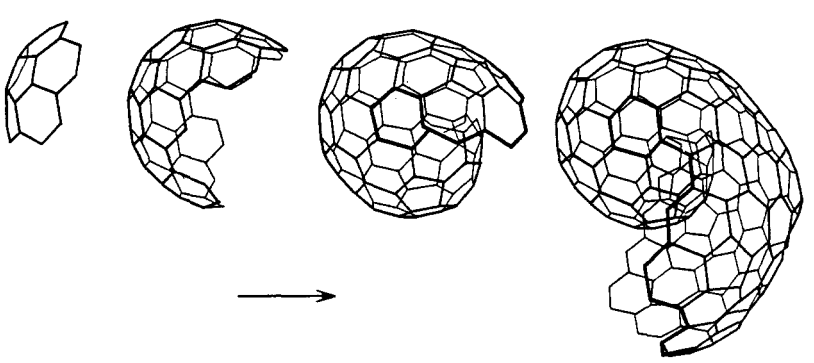

FIG. 6. Assembly of large clusters from hexagonal fragments at different stages of the process.[7]

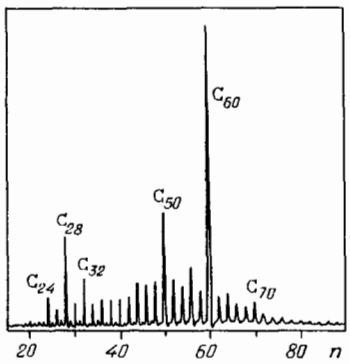


FIG. 7. A typical mass spectrum of the products of thermal vaporization.[21]

eter of 0.25 mm. The irradiation by laser of the tungsten band with the spray-coated layer of carbon condensate causes their stripping from the surface. An ArF-laser with a pulse energy of 200 $\mu$J and a beam diameter of 1.5 mm is used to ionize the particles. Mass spectra of the carbon condensate obtained in this manner at two values for the vaporization cell temperature are presented in Fig. 8. As is evident the $C_{60}$ cluster predominates in both cases; in addition, the $C_{70}$ cluster makes a noticeable contribution. The signals caused by the presence of the $C_{58}$, $C_{56}$, and $C_{54}$ clusters are hardly distinguishable. Argon was used as the buffer gas for the measurements.

A somewhat more complicated procedure for preparing a carbon condensate with a high $C_{60}$ content has been used in Refs. 25, 26, and 27. The processes of resistance heating and of thermal vaporization of a graphite rod in a helium atmosphere at 100 Torr pressure also served as the initial stage of this procedure. The carbon condensate which was formed here was carefully scraped off the collector surface and was drenched with benzene. A dark brown or black crystalline material is formed as a result of the subsequent drying of the suspension. Other nonpolar solvents such as $CS_2$ and $CCl_4$ were also successfully used instead of benzene. As the measurements show, the use of the suspension leads to a significant increase of the relative output of $C_{60}$ clusters. The procedure described enables one to produce up to 100 mg per day of carbon condensate with a high $C_{60}$ content at one facility. Typical mass spectra of the product that have been

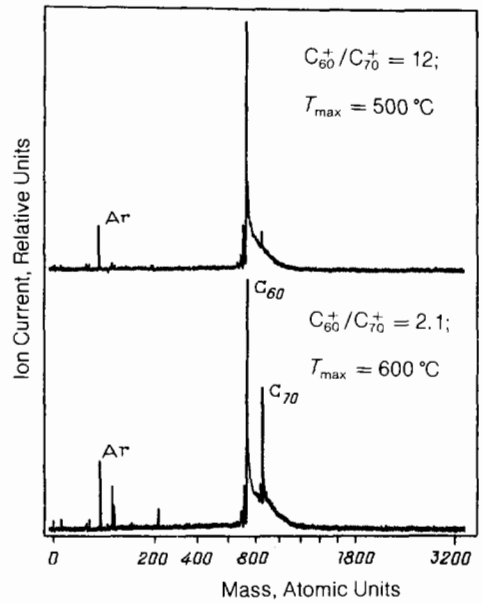


FIG. 8. A mass spectrum of clusters obtained by means of laser vaporization of a carbon condensate at different temperatures of the vaporization cell.[22]

obtained by means of a transit mass spectrometer are presented in Fig. 9. Pulverization of the condensate layer was achieved by irradiating it with a beam of 5 keV energy $Ar^+$ ions. Here the ion output ratio of $C_{70}^+$ to $C_{60}^+$ was $\sim 0.1$. Replacement of the $Ar^+$ ion beam by an electron beam led to a reduction of the value of this ratio to $\sim 0.02$. The same order of magnitude for this ratio is obtained by laser irradiation of a carbon condensate.[16,30] The technology described has received further development in Ref. 31, where a chromatographic procedure was used to separate the $C_{60}$ from a mixture of $C_{60}$ and $C_{70}$ clusters.

## 4. THE BREAKUP OF CARBON CLUSTERS

Useful information about the stability of carbon clusters follows from an analysis of the processes of destruction of these clusters. An investigation of the monomolecular breakup of carbon clusters with $n \geqslant 30$ shows that the stability of clusters with even values of $n$ significantly exceeds the stability of clusters with odd values of $n$. Here, both in the

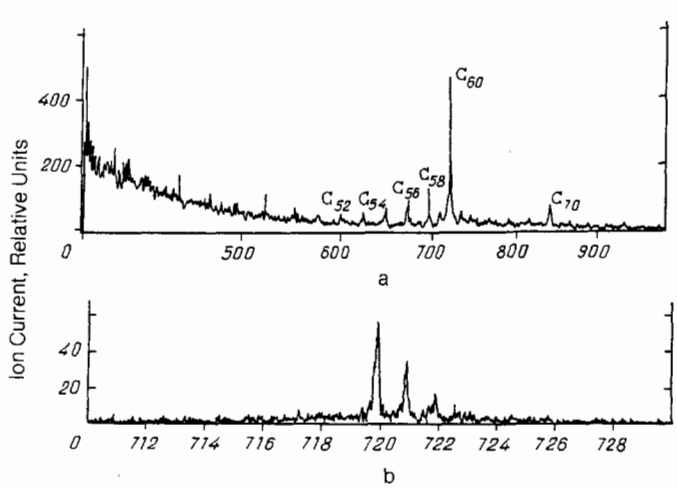


FIG. 9. A mass spectrum of carbon cluster ions that are formed during the vaporization of graphite electrodes in a helium atmosphere.[25] a) A low resolution spectrum. b) A high resolution spectrum; the peaks with $M = 721$ and $M = 722$ correspond to $C_{60}$ clusters with one and two atoms of the $^{13}C$ isotope.

TABLE I. The parameters which characterize the monomolecular breakup of $C_n^+$ clusters:[35] $C_n^+ \to C_{n-2}^+ + C_2$.

| $n$ | $K_d$, $10^{-4}$ sec | $\langle E_t \rangle$, eV | Fraction of broken-up clusters | $E_0$, eV | $E_{int}$, eV |
|---|---|---|---|---|---|
| 58 | 1,7 ± 0,5 | 0,4 ± 0,1 | 0,19 ± 0,02 | 4,5 ± 0,5 | 39 ± 2 |
| 60 | 0,7 ± 0,2 | 0,4 ± 0,1 | 0,10 ± 0,02 | 4,6 ± 0,5 | 39 ± 2 |
| 62 | 3,3 ± 0,5 | 0,3 ± 0,1 | 0,30 ± 0,02 | 3,0 ± 0,5 | 26 ± 2 |

case of monomolecular breakup[20] and also in the case of photodissociation,[32] the main channel for the breakup of $C_n$ molecules with even values of $n$ is associated with the splitting off of a $C_2$ fragment. This fact alone by itself evokes surprise, since the binding energy for a $C_2$ fragment is less than the corresponding value for $C_3$.[33] In the breakup of $C_n$ clusters (with odd $n$), the splitting off of a carbon atom is most probable. Thereby, the situation arises which favors the survival of clusters with even values of $n$, and the fraction of clusters with odd $n$ is no more than 1%.[32] The experimental facts quoted may serve as an indication of the structural features of $C_n$ clusters with large $n$ values, which are the absence of sharp angles and surfaces.[20,34–36]

Reference 35, where the energy spectra of the products of monomolecular breakup of $C_{58}$, $C_{60}$, and $C_{62}$ clusters have been measured, is devoted to investigating the indicated question in more detail. These measurements enabled one to estimate the energy of separation of a $C_2$ fragment from the clusters indicated above, and also the magnitude of the energy barrier which impedes their breakup. The cluster carbon ions that were created as a result of the laser irradiation of a graphite rod were accelerated in an electric field to energies $\approx 8$ keV, were gated according to their masses by means of a permanent magnet, and underwent monomolecular breakup in a chamber of one meter length free from the effect of external fields. The breakup products were analyzed with respect to mass and energy, and were detected by means of a photomultiplier. Processing of the energy spectra obtained here for the breakup products enabled one to determine values of the rate constant for monomolecular breakup $K_d$, the average value of the kinetic energy $\langle E_t \rangle$ that is released as a result of a breakup, the average value of the energy of separation $E_0$ of a $C_2$ fragment from the clusters indicated above, and the average value of the internal energy $E_{int}$ of a cluster. All these data are presented in Table I, where the values of the fractions of clusters of a given kind which broke up are also shown. As is evident, the value of the rate constant for breakup of a $C_{60}$ cluster is several times lower than the corresponding values for clusters with two atoms more or less.

Some idea of the mechanism of the breakup of a $C_{60}$ cluster and, consequently, of its structure, can be obtained based on an analysis of measurement results of the separation energy spectrum for the breakup products (in the center of mass coordinate system). The indicated results obtained on the basis of processing experimental data[35] are compared with the results of calculations made on the basis of model ideas about the structure of a $C_{60}$ cluster. As is evident from the comparison, the calculation results are slightly sensitive to the assumptions adopted about the structure of the cluster, and are determined principally only by the values of the internal energy of the cluster $E_{int}$ and the energy of separation $E_0$ of the $C_2$ fragment that are put into the calculation. This enabled one[35] to determine the values of the indicated parameters shown in Table I. In analyzing these values, the small difference of the energy characteristics of the $C_{60}^+$ and $C_{58}^+$ clusters which, in turn, differ significantly from the corresponding parameters of the $C_{62}^+$ cluster, catches the eye. This feature of the experimental data can serve as an indication of small structural differences of the $C_{60}^+$ and $C_{58}^+$ clusters. Here the increased content of $C_{60}^+$ clusters in the carbon dust finds a purely kinetic explanation connected with the relatively high probability of the process of destruction of heavier clusters, which is accompanied by the formation of $C_{60}^+$ clusters and, correspondingly, with the low probability for destruction of a $C_{60}^+$ cluster. However, one more explanation of the relation shown between the energy characteristics of the $C_{58}^+$, $C_{60}^+$, and $C_{62}^+$ clusters may be associated with the method for obtaining these clusters under the conditions of the experiment.[35] The high temperature of the graphite rod that is irradiated by high intensity laser radiation causes the

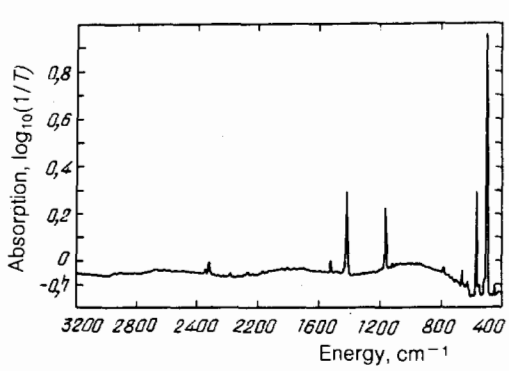


FIG. 10. The infrared absorption spectrum for a layer of $C_{60}$ clusters with $\sim 2\,\mu$m thickness spray-coated onto a transparent silicon substrate;[25,26] $T$ is the fraction of the radiation which passed through the substrate. The apparent negative absorption effect is caused by the reflection of radiation from the substrate.

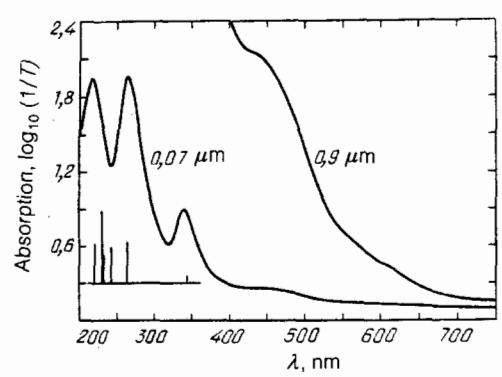


FIG. 11. The optical and ultraviolet absorption spectrum of spray-coated layers of $C_{60}$ clusters of different thicknesses coated onto a transparent quartz substrate.[25,26] The calculated results of the mutual positions and relative oscillator strengths for the resolved transitions of the $C_{60}$ cluster[37] are shown in the figure.

formation of carbon clusters with anomalously high internal energy content. It is possible that the structure of such clusters differs from the structure of particles that are formed as a result of the gas dynamical cooling of carbon dust particles in a buffer gas atmosphere. Obviously the question of the connection of the energy and kinetic characteristics of carbon cluster ions with their structural features requires further detailed explanation.

## 5. SPECTROSCOPY OF $C_{60}$

Spectroscopic research on the $C_{60}$ cluster serves as the main source of information about its structure. Thus, the meager nature of its infrared absorption spectrum is a direct indication of the high level of symmetry of $C_{60}$. Typical absorption spectra for infrared and visible radiation from carbon dust coated in a thin layer onto a transparent quartz plate are presented in Figs. 10 and 11.[25,26 3)] Four strong absorption lines with centers at energies of 1429 $cm^{-1}$, 1183 $cm^{-1}$, 577 $cm^{-1}$, and 528 $cm^{-1}$ and with widths varying in the range from 3 $cm^{-1}$ to 10 $cm^{-1}$ are detected in the spectrum. On the spectra of specimens made from the $^{13}C$ isotope with a 99% degree of purification, the absorption lines are shifted to the red. The values of the absorption frequencies shown above approximately conform to the results of calculations[38–42] made on the assumption that the $C_{60}$ structure is a truncated icosahedron.

The high symmetry of the $C_{60}$ cluster appears also in the richness of the Raman scattering spectrum of these molecules. The results of a detailed investigation of the indicated spectra are presented in Ref. 22, where an argon ion laser with $\lambda = 514$ nm and an output power of 140 $\mu$W, and whose beam was focused into a spot of 13 $\mu$m diameter, was used as the source of radiation. Here the radiation of the Raman frequencies scattered in the direction opposite to the pumping radiation was recorded. The spectral resolution was $\approx 9$ $cm^{-1}$. Typical Raman scattering spectra for carbon dust coated onto tungsten foil are presented in Fig. 12. The specimens that are investigated have been prepared according to the procedure described in the previous section[22] and are characterized by the mass spectra presented in Figs. 12a and 12b, respectively. The main difference in the spectra presented in Figs. 12a and 12b is associated with the different relative abundance of $C_{70}$ clusters in the specimens. The lines with the frequencies 1568 $cm^{-1}$, 1232 $cm^{-1}$, 1185 $cm^{-1}$, 1062 $cm^{-1}$, and 260 $cm^{-1}$ that are observed in the spectrum of Fig. 12b with a higher relative $C_{70}$ content are attributed to this cluster. The lines with the frequencies 1469 $cm^{-1}$, 497 $cm^{-1}$, and 273 $cm^{-1}$ that are observed in these spectra are attributed to the $C_{60}$ cluster.

The frequencies, relative intensities, and identifications of the Raman scattering lines of soot shown in Fig. 12 are presented in Table II. The results of measuring the depolarization $\rho = I_{\perp}/I_{\parallel}$, where $I_{\perp}$ and $I_{\parallel}$ are the intensities of the scattered radiation of the corresponding Raman frequency with the polarizations perpendicular to and parallel to the polarization of the incident radiation, are also shown for the strongest lines. The high degree of polarization of the scattered radiation which characterizes the two strongest $C_{60}$ lines (497 $cm^{-1}$ and 1469 $cm^{-1}$) indicates that the indicated lines are connected with completely symmetric types of vibrations of this molecule.

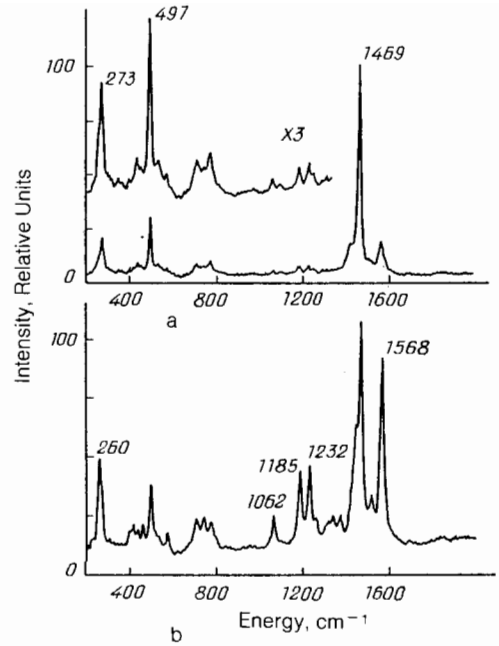


FIG. 12. Raman scattering spectra of a carbon condensate coated onto tungsten foil.[22] a) The temperature of the vaporization cell is $T_c = 500$ °C; b) $T_c = 600$ °C.

It is interesting to note that the value of the Raman frequency $\nu = 273$ $cm^{-1}$ found experimentally[22] is in surprising agreement with the results of calculations made considerably before the indicated experiment was performed. According to these calculations, the vibration frequency of a truncated icosahedron at which a sphere is converted into an ellipsoid (the "pumpkin" mode $H_g$) equals $273 \pm 10$ $cm^{-1}$,[25–29] and moreover, the indicated scatter is the result of statistical averaging of data from different authors. The frequency values 1469 $cm^{-1}$ and 497 $cm^{-1}$ have somewhat worse agreement with the calculations; these are attributed to completely symmetric types of vibrations. The calculated values of the indicated frequencies, the first of which corresponds to the stretching and compression of the pentagonal surfaces of an icosahedron and the second to "breathing" vibrations, are in the ranges from 1627 $cm^{-1}$ to 1830 $cm^{-1}$ and from 510 $cm^{-1}$ to 660 $cm^{-1}$, respectively.

## 6. SOOT AND THE $C_{60}$ CLUSTER

A complicated process of chemical transformations occurs for organic compounds in a combustion flame, such that carbon dioxide and water are the end products of these processes. However, at an intermediate stage of these processes, various clusters and radicals, also including the $C_{60}$ cluster, can be formed in the flame.[43,44] It is clear that these intermediate compounds affect the properties of the flame, for they determine the chemical transformation rates and the energy balance in the flame. In particular, an analysis of the optical properties of a candle flame[45,46] shows that an appreciable part of the organic material forms soot at an intermediate stage of the process. Actually, the radiation power of a transparent flame is proportional to the mass of the soot which is located in it, and is independent of the masses of the soot particles. Therefore, on the basis of the measured radiative parameters of a flame, one can estimate the mass of soot which is located in the flame and compare it

TABLE II. The Raman frequencies, relative intensities, and depolarization coefficients for the Raman scattering lines of carbon dust.[22] The values of $I_a$ and $I_b$ correspond to the conditions of Figs. 9a and 9b.

| $\nu$, cm$^{-1}$ | $I_a$ | $I_b$ | $\rho(\pm 0{,}02)$ | Identification |
|---|---|---|---|---|
| 260 | 7 | 34 | | $C_{70}$ |
| 273 | 17 | 17 | | $C_{60}$, $H_g$ |
| 413 | | 9 | | |
| 435 | 5 | 6 | | |
| 457 | | 9 | | |
| 497 | 27 | 27 | 0,16 | $C_{60}$, $A_g$ |
| 571 | 2 | 9 | | |
| 705 | | 13 | | |
| 711 | 4 | | | |
| 739 | | 13 | | |
| 773 | 6 | 13 | | |
| 1062 | 2 | 14 | 0,23 | $C_{70}$ |
| 1185 | 4 | 34 | 0,19 | $C_{70}$ |
| 1232 | 4 | 36 | 0,19 | $C_{70}$ |
| 1336 | | 11 | | |
| 1370 | | 11 | | |
| 1430 | 13 | | | |
| 1448 | | 32 | | |
| 1469 | 100 | 100 | 0,11 | $C_{60}$, $A_g$ |
| 1513 | 3 | 15 | | |
| 1568 | 15 | 88 | 0,24 | $C_{70}$ |

with the mass of the organic material taking part in the process. Such a comparison also shows that an appreciable part of the organic material is found in the flame in the form of soot particles, which also emit radiation.

These soot particles are formed in a candle flame in a chemical reaction with the participation of molecules of stearene $C_{18}H_{36}O$. It is clear that such complicated molecules can start the formation of clusters with a large number of atoms. Another conclusion is also possible: the flames of organic compounds containing large molecules are used as radiation sources. The flames of simple organic compounds (methane, alcohol) are characterized by low light output (the ratio of luminosity to thermal power), for in this case the efficiency of forming large clusters, these of soot particles which emit radiation, is low.

If the soot particles in a flame are $C_{60}$ clusters, then this will show up in the properties of the flame. These clusters do not have resolved radiating transitions in the optical spectral region, so that a flame which contains them will be fainter than with other soot particles present. At the same time, the radiation of a flame in the infrared spectral region is fairly efficient due to $C_{60}$ clusters, especially in a case that vibrationally excited clusters are formed under nonequilibrium conditions. If the properties of a flame depend on the rate of a chemical reaction for oxidizing carbon, then the presence of $C_{60}$ clusters will retard this process because of the chemical inertness of the cluster. Then $C_{60}$ clusters which are located in a flame will lead to a reduction of its temperature.

Obviously, the nature of the formation of $C_{60}$ clusters in a flame is the same as under other conditions, including astrophysical ones.[7] It consists of joining new rings, pentagons or hexagons, to the elements of a cluster. As a result of this process, various clusters of carbon with closed shells can be formed, also including $C_{60}$.

The analysis made shows that the $C_{60}$ cluster may be one of the varieties of soot that is present in a flame of organic compounds. The properties of the flame in this case are different from those which are created by other soot particles. The presence of the clusters in a flame can be recorded by the radiation of the flame in the lines at 1429 cm$^{-1}$, 1183 cm$^{-1}$, 577 cm$^{-1}$, and 528 cm$^{-1}$, which correspond to the strongest transitions of the $C_{60}$ cluster. The process of forming soot in a flame and its cluster structure were investigated in detail in Ref. 43, where a disk burner with a 75 mm diameter placed in a chamber at reduced pressure was used. Flames of benzene $C_6H_6$ and acetylene $C_2H_2$, burning at different C/O concentration ratios, served as the object of the investigation. A cold mixture of the hydrocarbon with oxygen was supplied to the burner at 300 K temperature and 20 Torr pressure with velocities varying from 35 cm/sec to 60 cm/sec. The burner ended in an exit aperture of 0.8 mm diameter, which served to form a supersonic flow of fuel. The flame propagated in a vacuum chamber, where a pressure of $\sim$0.001 Torr was maintained by means of pumps. Quartz probes with platinum coatings were used to remove ions from different points of the flame. The ion mass spectrum was investigated by means of a transit mass spectrometer.

As detailed investigations showed, the intensive formation of carbon clusters with three-dimensional structure occurs even at distances greater than 2 mm from the edge of the burner. A typical mass spectrum of positive $C_n^+$ cluster ions that has been obtained in a benzene flame with a C/O = 0.76 ratio at a fuel supply velocity to the burner of 42 cm/sec, with gas removal at 15 mm distance from the edge of the burner, is presented in Fig. 13.[43] The mass spectrometer signal is presented in units of the concentrations of the corresponding particles in the flame. One must note that the spectrum presented is significantly different from a spectrum of negatively charged clusters, among which the clusters $C_{50}^-$ and $C_{82}^-$ characterize the highest concentrations, whereas the $C_{60}^-$ cluster has concentrations ranking among the twentieth or thirtieth places in decreasing order. The mass spectra of carbon clusters in acetylene and benzene flames have just the same qualitative features, however, the acetylene flame is somewhat richer in the larger clusters than the benzene flame.

As is evident from the data presented in Fig. 13, the

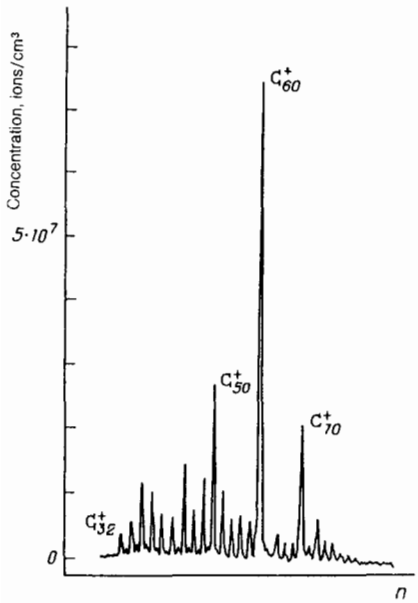


FIG. 13. A mass spectrum of positive carbon cluster ions obtained in a benzene flame with the $[C]/[O] = 0.76$ ratio at a fuel supply velocity to the burner of 42 cm/sec, with gas removal at 15 mm from the edge of the burner.[43]

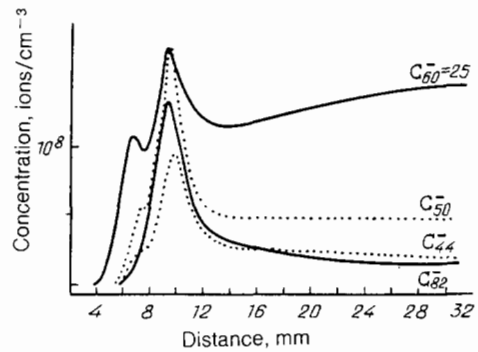


FIG. 14. Dependence of the concentrations of negative carbon cluster ions on distance from the edge of the burner in a benzene flame.[43]

mass-spectrum of the carbon clusters in hydrocarbon flames agrees qualitatively with the mass-spectrum of the clusters that are observed during the thermal pulverization of graphite (see Fig. 7). One must consider the absence of $C_{2n}H$ type compounds as one more distinctive feature of the mass spectra of clusters. Only clusters having an odd number of carbon atoms contain hydrogen ($C_{2n+1}H$).

The results presented in Fig. 14 of measuring the spatial dependences of the concentrations of different negatively charged carbon clusters in a benzene flame give a good idea of the kinetics of clustering and the formation of soot in a hydrocarbon flame.[43] As is evident, the concentrations of $C_{50}^-$, $C_{44}^-$, and $C_{82}^-$ clusters, which have their maximum values near the edge of the burner, decrease sharply as one moves away from the edge of the burner, whereas the concentration of $C_{60}^-$ clusters continues to increase monotonically as one moves away from the edge of the burner. This indicates the $C_{44}$, $C_{50}$, and $C_{82}$ clusters as intermediate products of clustering, the final product of which obviously is the more stable $C_{60}$ cluster.

The research carried out in the cited Ref. 43 indicates a high temperature sensitivity of the soot formation processes in hydrocarbon flames. Thus, a temperature increase by 200 K leads to a reduction of the concentration of positively charged $C_{60}^+$ clusters by approximately an order of magnitude. The flame temperature corresponding to the maximum concentration of clusters with regular polyhedral structures is approximately 2100 K.

## 7. MACROSTRUCTURES CONSISTING OF $C_{60}$ CLUSTERS

Since one can successfully separate $C_{60}$ clusters from a carbon vapor and precipitate them onto a substrate, suitable structures, which are surface and three-dimensional crystals can be formed from these clusters. This is a step towards obtaining a new, stable form of carbon. Such research is starting at present, so that one may expect that it will have reached a new level at the time this review is published.

The structures under consideration consist of interacting $C_{60}$ clusters. The investigations carried out in Refs. 47 and 48 showed that systems consisting of $C_{60}$ clusters on a substrate have a regular structure over small sections. Thus, in Ref. 47, $C_{60}$ clusters were precipitated onto gold foil and they formed a regular structure on it with a distance $r = 1.10 \pm 0.05$ nm between neighboring clusters. A mass-spectroscopic analysis, Raman scattering, and an analysis based on nuclear magnetic resonance show that, along with the $C_{60}$ clusters, there turns out to be a definite fraction of $C_{70}$ clusters on the substrate, which evidently disrupt the regular structure over large distances.

Let us analyze the properties of a two-dimensional crystal by using the analogy of the cluster under consideration with graphite. Assuming that the distance between the nearest planes of two clusters in a crystal is the same as the distance between neighboring layers of graphite (0.335 nm),[28,29] we find that the distance between the centers of neighboring clusters is 1.08 nm. As is evident, this value agrees with the measured value within the limits of its accuracy.

Obviously, one can form a three-dimensional lattice from $C_{60}$ clusters. Considering, as a first approximation, these clusters as spheres, one must choose one of the lattices that is densely packed as a crystalline lattice. A face centered cubic lattice, in which each cluster has 12 neighbors, is the most suitable one among them. Then the contacts between neighboring clusters are made through the pentagons of their structure. Using the analogy with graphite, for which the atoms of neighboring layers are displaced by half the

TABLE III. The ratio of the average vibrational energy of an inert gas diatomic molecule at the melting temperature of the inert gas to the dissociation energy of a molecule.

| Element | Ne | Ar | Kr | Xe |
|---|---|---|---|---|
| The Ratio | 0,29 | 0,30 | 0,30 | 0,29 |

TABLE IV. The parameters of carbon crystals.

| Type | Diamond | Graphite | Cluster |
|---|---|---|---|
| Density, g/cm$^3$ | 3,51 | 2,23 | 1,3 |
| Melting Temperature, $K$ | *) | 4120 ± 50 | 510 ± 20 |

*) It transforms into graphite at a temperature about 4000 K.

lattice constant, one must note that, in this case too, the vertices of the contact pentagons must be pointing in different directions. This means that the line joining the centers of neighboring clusters passes through the centers of the contact pentagons, and the atoms forming the vertices of these pentagons are turned at an angle of $\pi/5$ radians with respect to each other in planes that are perpendicular to the axis joining their centers.

Let us determine the density of the carbon in the crystal under consideration. It equals $\rho = 60m\sqrt{2}/r^3$, where $m$ is the mass of a carbon atom, and $r$ is the distance between the nearest clusters. Assuming $r = 1.08$ nm, we shall find $\rho = 1.3$ g/cm$^3$. As is evident, this form of crystalline carbon, consisting of $C_{60}$ clusters, is less dense than other forms of graphite and diamond.

Other parameters of the crystalline lattice under consideration and, first of all, the melting temperature of such a crystal, are of interest. This parameter will enable one to understand the conditions for the existence of the crystal. To determine this value, we pursue further the analogy with graphite. The energy of breaking the bond between neighboring layers which is evaluated per carbon atom is 0.077 eV in graphite.[49] We shall assume that the same energy binds the carbon atoms entering into the makeup of pentagonally neighboring clusters.

To determine the melting temperature of this crystal, we use an analogy with crystals of an inert gas. Here we shall assume that, at the melting temperature, a definite degree of vibrational excitation is reached which is in some relation to the binding energy between the elements of the crystal. Let us pick out a diatomic molecule of an inert gas and let us determine the ratio of the average vibrational energy to the dissociation energy at the melting temperature.[50] The corresponding values are shown in Table III; the average value of this ratio is 0.29. Using the same ratio for a crystal consisting of the carbon clusters under consideration, we shall find $T_{melt} = 510 \pm 20$ K for the melting temperature of this crystal. This value is comparable with the value $> 550$ K shown in the experimental paper of Ref. 31.

Thus, a crystal consisting of $C_{60}$ clusters is a new form for the existence of condensed carbon. The elements of its structure are the same as for graphite, and the technology to obtain such crystals can be connected with the processing of graphite. Characteristics of the crystalline forms of carbon are presented in Table IV.

Interest in investigating structures consisting of $C_{60}$ clusters increased significantly after the appearance of Refs. 51 and 52 in print, in which the results have been discussed of measurements of the conductivities of structures of the type $A_xC_{60}$ (A is an alkali metal). The indicated structures have been obtained as a result of exposing $C_{60}$ films or polycrystalline specimens of $C_{60}$ to metal vapors at temperatures of several hundred degrees Celsius.[51] The report in Ref. 52 on the observation of superconductivity for $K_xC_{60}$ compounds at temperatures up to 18 K caused a genuine sensation among specialists in the field of superconductivity. The value quoted for the critical temperature is a record for molecular superconductivity. For instance, the critical temperature which characterizes the superconductivity of graphite alloyed with potassium is 0.55 K.[53]

Results of measuring the temperature dependence of the specific intensity of magnetization of a $K_3C_{60}$ superconducting specimen that has been done by means of a SQUID magnetometer[52] are presented in Fig. 15. The specimen investigated was prepared as a result of the chemical reaction of 29.5 mg of $C_{60}$ with 4.8 mg of potassium, which went on for 36 hours at $T = 200$ °C. Cooling of the specimen was carried out by turning on ($FC$) and turning off ($ZFC$) the magnetic field. The shape of the curves indicates the presence of a strong Meissner effect, indicating superconductivity of the specimen at temperatures below 18 K.

The critical temperature of a $K_xC_{60}$ superconducting film measured on the basis of the temperature dependence of the conductivity of the film turned out to equal 7 K. The film thickness was 960 Å, and the mass of the specimen was 0.5 mg. The authors of Ref. 52 express confidence that optimizing the composition and improving the technology for preparing $A_xC_{60}$ type structures will lead to further improvement of the superconducting properties of these materials.

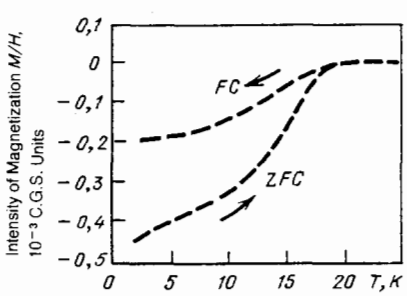


FIG. 15. The temperature dependence of the intensity of magnetization for a $K_xC_{60}$ superconducting specimen.[52] Cooling of the specimen was carried out in the presence of the magnetic field ($FC$) and with field switched off ($ZFC$).

## 8. CONCLUSION

The information presented shows that a $C_{60}$ carbon cluster turns out to be distingushable among other carbon clusters. It is essentially a hypermolecule with low reactivity, which enables one to single out these clusters and to carry out different operations on them, including collecting them on a substrate. Thus, a $C_{60}$ carbon cluster is a stable form of carbon which can be used to obtain new materials and new chemical compounds. This opens possibilities for developing a whole series of applications based on high-precision physical methods.

[1)] The term "cluster" (or clump, bunch, or bundle in English) is used for different systems of bound particles. In this review, this term refers to a system of bound atoms.

[2)] Compounds of the $C_6H_6$ type, *et al.*, are analogs of these structures in organic chemistry.

[3)] Let us also refer to Ref. 54, where luminescence spectra have been obtained for a $C_{60}$ film at $T = 20$ K in the 700 nm$\leqslant\lambda\leqslant$1100 nm range, and to Ref. 55, where an emission spectrum was observed for $C_{60}$ molecules in the gaseous phase in the 500 cm$^{-1}\leqslant\nu\leqslant$2000 cm$^{-1}$ range, which corresponds to the far infrared range.


[1] A. V. Eletskii and B. M. Smirnov, Usp. Fiz. Nauk **159**, 45 (1989) [Sov. Phys. Usp. **32**, 763 (1989)].
[2] P. Jena, B. K. Rao, and S. N. Hanna (Eds.), *Physics and Chemistry of Small Clusters*, Plenum, N.Y.; London, 1987.
[3] A. Ding and J. Hesslich, Chem. Phys. Lett. **94**, 54 (1983).
[4] O. Echt, K. Sattler, and E. Recknagel, Phys. Rev. Lett. **47**, 1982 (1982).
[5] O. Echt *et al.*, Bunsenges. Phys. Chem. **86**, 860 (1982).
[6] E. Recknagel, Bunsenges. Phys. Chem. **88**, 201 (1984).
[7] H. Kroto, Science **242**, 1139 (1988).
[8] R. F. Curl and R. E. Smalley, Science **242**, 1017 (1988).
[9] E. Osawa, Kogaku, Kyoto (Japan) **25**, 854 (1970). (In Japanese).
[10] Z. Ioshida and E. Ozawa, Aromaticity [in Japanese], Kyoto, 1971.
[11] D. A. Bochvar and E. G. Gal'pern, Dokl. Akad. Nauk SSSR **209**, 610 (1973) [Dokl. Chem. **209**, 239 (1973)].
[12] I. V. Stankevich, M. V. Nikerov, and D. A. Bochvar, Usp. Khim. **53**, 1101 (1984). [Russ. Chem. Rev. **53**, 640 (1984)].
[13] R. A. Davidson, Theo. Chim. Acta **58**, 193 (1984).
[14] A. D. J. Haymet, J. Am. Chem. Soc. **108**, 319 (1986).
[15] H. W. Kroto *et al.*, Nature **318**, 162 (1985).
[16] Q. L. Zhang *et al.*, J. Phys. Chem. **90**, 525 (1986).
[17] A. Kaldor *et al.*, Z. Phys. **3**, 195 (1986).
[18] A. O'Keefe, M. M. Ross, and A. P. Baronovski, Chem Phys. Lett. **130**, 17 (1986).
[19] M. Y. Hahn *et al.*, Chem Phys. Lett. **130**, 12 (1986).
[20] S. C. O'Brien *et al.*, Chem. Phys. Lett. **132**, 99 (1986); J. Chem. Phys. **88**, 220 (1988).
[21] D. M. Cox, K. C. Reichmann, and A. Kaldor, J. Am. Chem. Soc. **110**, 1588 (1988).
[22] D. S. Bethune *et al.*, Chem. Phys. Lett. **179**, 219 (1990).
[23] G. Meijer and D. S. Bethune, J. Chem. Phys. **93**, 7800 (1990).
[24] R. D. Johnson, G. Meijer, and D. S. Bethune, J. Am. Chem. Soc. **112**, 8983 (1990).
[25] W. Kratschmer *et al.*, Nature **347**, 354 (1990).
[26] W. Kratschmer, K. Fostiropoulos, and D. R. Huffman, Chem. Phys. Lett. **170**, 167 (1990).
[27] W. Kratschmer, K. Fostiropoulos, and D. R. Huffman, *Dusty Objects in the Universe* (E. Bussolettu and A. A. Cittone (Eds)), Amsterdam, 1990, p. 89.
[28] E. E. Flint, *Nachala Kristallegrafii* (*the origins of crystallography*), Vysshaya Shkola, M., 1961.
[29] V. S. Veselovskiĭ, Grafit (Graphite) (In Russian) M., 1960.
[30] H. W. Kroto *et al.*, Nature **329**, 529 (1987).
[31] J. P. Hare, H. W. Kroto, and R. Taylor, Chem. Phys. Lett. **177**, 394 (1991).
[32] P. P. Radi *et al.*, J. Chem. Phys. **88**, 2809 (1988).
[33] K. Raghavachari and S. Binkey, J. Chem. Phys. **87**, 2191 (1987).
[34] F. D. Weiss *et al.*, J. Am. Chem. Soc. **110**, 4464 (1988).
[35] P. P. Radi *et al.*, Chem. Phys. Lett. **174**, 223 (1990).
[36] P. P. Radi *et al.*, J. Chem. Phys. **92**, 4817 (1990).
[37] S. Larsson, A. Volosov, and A. Rosen, Chem. Phys. Lett. **137**, 291 (1987).
[38] Z. Slanina *et al.*, J. Mol. Struct. Thermochem. **202**, 169 (1989).
[39] D. E. Weeks and W. G. Harter, J. Chem. Phys. **90**, 4744 (1989).
[40] R. E. Stanton and M. D. Mewton, J. Phys. Chem. **92**, 2141 (1988).
[41] S. J. Cyvin *et al.*, Chem. Phys. Lett. **143**, 377 (1989).
[42] Z. C. Wu, D. A. Jelski, and T. F. George, Chem. Phys. Lett. **137**, 291 (1987).
[43] P. H. Gerhardt, S. Loffer, and K. H. Homann, Chem. Phys. Lett. **137**, 306 (1987).
[44] B. D. Crittenden and R. Long, Combustion and Flame **20**, 359 (1973).
[45] L. A. Luizova, B. M. Smirnov, and A. D. Khakhaev, Dokl. Akad. Nauk SSSR **309**, 1359 (1989) [Sov. Phys. Dokl. **34**, 1086 (1989)].
[46] L. A. Luizova *et al.*, Teplofiz. Vys. Temp. **28**, 897 (1990). [High Temp. (USSR) **28**, 674 (1990)].
[47] R. J. Wilson *et al.*, Nature **348**, 621 (1990).
[48] J. L. Wragg *et al.*, Nature **348**, 623 (1990).
[49] R. J. Good *et al.*, J. Phys. Chem. **62**, 1418 (1958).
[50] Landolt-Bornstein Vol. 6, Springer-Verlag, Berlin; Heidelberg, N.Y., 1971.
[51] R. C. Heddon *et al.*, Nature **350**, 320 (1991).
[52] A. F. Hebard *et al.*, Nature **350**, 600 (1991).
[53] N. B. Hannay *et al.*, Phys. Rev. Lett. **14**, 225 (1965).
[54] S. Reber *et al.*, J. Phys. Chem. **95**, 2127 (1991).
[55] C. I. Frum *et al.*, Chem. Phys. Lett. **176**, 504 (1991).


Translated by Frederick R. West